RAPID COMMUNICATIONS

PHYSICAL REVIEW B VOLUME 42, NUMBER 2 15 JULY 1990-I

Interactions between extended and localized states in superlattices

F. Agulló-Rueda,* E. E. Mendez, H. Ohno,† and J. M. Hong
IBM Research Division, Thomas J. Watson Research Center, P.O. Box 218, Yorktown Heights, New York 10598
(Received 7 May 1990)

We have observed electric-field-induced interactions between the extended states of a (40 Å)-(15 Å) GaAs-$Ga_{0.65}Al_{0.35}As$ superlattice and the localized state of an 80-Å terminating GaAs well. At fields such that the energy of an extended state was close to that of the localized level, low-temperature (5-K) photocurrent spectra associated with interband transitions exhibited three pronounced doublets of peaks with characteristic resonant and anticrossing behavior. As the two levels approached each other, the initially asymmetrical peak intensities first became of comparable strengths and then exchanged their roles in the resulting asymmetrical peak intensities as the states repelled each other. A comparison of the experimental results with numerical solutions of Schrödinger's equation showed that the doublets result from the interaction of the localized state with the three superlattice states of highest energy, centered around its last three wells.

The electronic structure of a superlattice consists of energy bands originating from the interaction among the states of its quantum-well constituents. This similarity to energy bands in conventional crystals and the ability to mimic them in a controlled way makes superlattices ideal for the study of selected properties of solids. An open question currently being investigated using superlattices is the effect of a terminating crystalline periodicity at the end of a real solid, important for a deeper understanding of surface states.

The periodic potential of the superlattice can be interrupted by making one of the end quantum wells different from the rest, e.g., by a higher confinement barrier. This situation is analogous to an ideal surface as proposed long ago by Tamm,[1] which we have considered in detail recently.[2] By terminating a $GaAs/Ga_{1-x}Al_xAs$ superlattice with an AlAs layer, which provides potential barriers for electrons and holes higher than those of the superlattice, we have shown experimentally the formation of a state localized in the last well (Tamm state), whose energy is above the superlattice miniband. On the other hand, if the terminating barrier is lower, or the last well is wider, than the rest, that localized level would be below the miniband.

In this paper we focus on the case in which the periodicity is destroyed by a wider well at the end of an otherwise ideal superlattice. Taking advantage of the tunability offered by an electric field, we demonstrate that the extended states of the superlattice can penetrate into the "last" well—interacting and mixing with its localized state—provided that the energy differences between the former and the latter are not too large. The potential profile we consider is sketched in Fig. 1, where the last (leftmost) well of a superlattice has a width double ($2d$) that of all the others. Although, strictly speaking, the rupture of the periodicity affects all the quantum states, its effects are largest at the last well. In a tight-binding scheme the electronic coupling between wells depends on the energy difference and wave-function overlap among the respective isolated-well states. As the eigenenergy of the last well, when considered isolated, is significantly

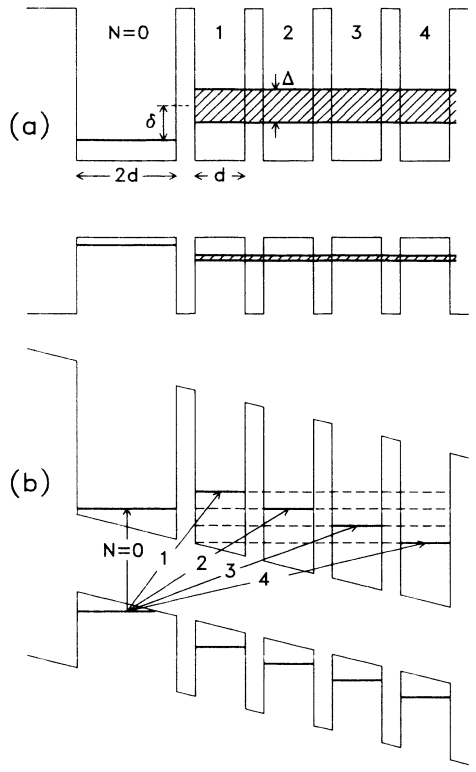

FIG. 1. Schematic potential profile for a structure consisting of a finite (40 Å)/(15 Å) GaAs/$Ga_{0.65}Al_{0.35}As$ superlattice with the last (leftmost) well doubled in width relative to all others. For simplicity, excited states of the last well and light-hole levels are not shown. (a) In the absence of an electric field the state in the last well is localized, while those in the superlattice miniband (represented by a shadowed area) are extended. (b) Under an electric field the miniband is split into a set of states (Stark ladder), which for some resonant fields interact strongly with the localized level. The vertical arrow indicates an interband transition between the localized hole and electron states of the last well ($N=0$). The other arrows represent transitions between the localized hole state and the Stark-ladder electron states ($N=1,2,3,4$).

 © 1990 The American Physical Society

lower than that of all the others, its coupling to them (as determined by their energy difference δ) will be largely reduced. To first approximation, this state will not participate in the miniband formation and will remain localized. However, a picture that completely ignores the interaction between the last well and the rest of the superlattice is oversimplified, and it does not adequately describe the energy structure of the combined system.

A convenient way of studying that interaction is by applying an electric field, $\mathcal{E}$, along the superlattice axis, which allows a continuous variation of the parameter δ. Although, semiclassically the field can be seen as producing a tilting of the miniband, quantum mechanically the miniband breaks under the field into a Stark ladder of states [see Fig. 1(b)] whose wave functions gradually lose their extended character and whose energy separation is $ne\mathcal{E}D$, where D is the superlattice period and $n=1,2,3,\ldots$ (Ref. 3). Whenever one of these states is aligned in energy with the localized state of the last well, their mutual interaction is enhanced resonantly and the latter becomes extended. It is easy to demonstrate that in the weak-coupling limit the resonant electric fields, $\mathcal{E}_n$, are given by

$$\mathcal{E}_n \simeq \frac{\delta}{ND+d/2} . \tag{1}$$

N is the neighbor order of the superlattice wells relative to the last well ($N=1$ for the nearest neighbor, $N=2$ for the second-nearest neighbor, and so on). As an example, for a 55-Å-period superlattice consisting of 40-Å GaAs wells and 15-Å $Ga_{0.65}Al_{0.35}As$ barriers, δ for an 80-Å last well is 63.9 meV and the resonant fields would be 34.5, 49.2, and 85.2 kV/cm, for $N=3,2,1$, respectively.[4]

We have observed optically these interactions up to the third-nearest neighbor, by means of photocurrent (PC) spectroscopy, a technique frequently used to study interwell resonances in coupled double quantum wells.[5-8] The potential profile of Fig. 1 was realized on a heterostructure, grown by molecular-beam epitaxy on an n^+-type doped GaAs(100) substrate, that consisted of a 25-period, undoped (40 Å)-(15 Å) GaAs-$Ga_{0.65}Al_{0.35}As$ superlattice terminated by an 80-Å last well. To reduce carrier leakage, the structure was finished on both ends by 600-Å $Ga_{0.65}Al_{0.35}As$ barriers.

A uniform electric field was applied to the heterostructure by a voltage between the n^+-type substrate and a p-type GaAs cladding layer on top. Under reverse bias the electric field in the intrinsic region is given by $\mathcal{E} \simeq (V-V_b)/W$, where V is the applied voltage, V_b the built-in voltage, and W the width of the intrinsic region. A numerical integration of Poisson's equation yielded $V_b \simeq 1.6$ V, and an almost linear $\mathcal{E}$-V relationship. Interband optical transitions were studied at 5 K using an LD700-dye laser pumped by a Kr-ion laser. The power density on the sample was kept below 0.3 W/cm^2 to avoid screening of the external field by the photoinduced carriers. The PC spectra were corrected by the laser power for each energy.

For a configuration like the one illustrated in Fig. 1(b) the PC spectra are very rich in structure, due to the many possible interband transitions. We concentrate here on transitions from valence-band states in the last well to conduction-band states centered in the last ($N=0$) and adjacent ($N=1,2,3,\ldots$) wells of the superlattice. In Fig. 2 we have plotted selected spectra for various fields in the region around the $N=3$ resonance, where the transitions could be followed more clearly. At fields corresponding to the other two resonances ($N=2$ and $N=1$), the spectra, not shown, exhibited similar patterns.

Two doublets of peaks can be identified in Fig. 2, representing the heavy-hole (low energy) and light-hole (high energy) transitions. At low fields, the strong and weak peaks of each pair correspond to the $N=0$ and 3 transitions, respectively. The intensity of the $N=0$ peak reflects the large overlap between the strongly localized electron and hole wave functions in the last well. On the other hand, the weakness of the $N=3$ feature is a consequence of the small penetration in the last well of the electron wave function centered in the third well. This state, originally fully extended, is gradually localized by the electric field while its energy decreases relative to the last well.

With increasing field, each doublet shows a characteristic resonant behavior: asymmetrical intensities when the two peaks are far apart, changing into peaks of comparable strengths as they approach each other, and then exchanging their roles in the final asymmetrical intensities. In a tight-binding scheme, the interaction and mixing between the two electron states produce energy repulsion and comparable peak intensity, as the two have a large probability density both in the $N=0$ and the $N=3$ wells. The lower (higher) -energy state corresponds to the symmetric (antisymmetric) combination of the noninteracting states.

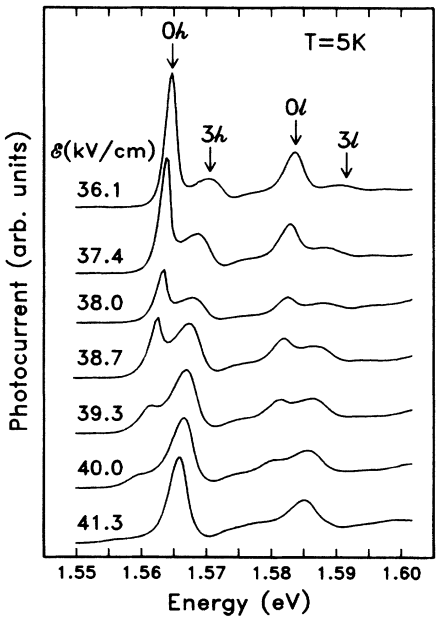

FIG. 2. Selected photocurrent spectra at various electric fields taken at 5 K for a heterostructure as the one shown in Fig. 1. The energy interval and the range of electric fields correspond to the anticrossing resonance between the localized electron and third Stark-ladder electron levels. Similar resonances were observed for the second and first Stark-ladder states.

A plot of the peak energies for the three resonances as a function of field (see Fig. 3) reveals the existence of level anticrossing at 30.5, 48.8, and 97.4 kV/cm, and even hints a fourth resonance at 25.6 kV/cm. The parallelism between the heavy- and light-hole transitions [separated for clarity in Figs. 3(a) and 3(b), respectively] shows that the resonances occur for states in the conduction band. The minimum energy splitting between the two peaks of each doublet reflects the magnitude of the interaction (or, equivalently, the overlap) between the state of the last well and the corresponding Stark-ladder state. From Fig. 3, the measured minimum splittings are 4.57, 11.9, and 29.0 meV, for the third, second, and first Stark states, respectively. A vestige of this kind of interactions (although for higher N) appeared in recent studies of optical transitions between the discrete levels of a 102-Å quantum well imbedded in a 36-Å-period superlattice,[9] where kinks in a plot of the transition energies versus electric field were attributed to the crossing of the Stark-ladder states of the superlattice with the quantum-well levels. However, the extremely small interaction between them prevented the observation of any anticrossing gap.

The experimental anticrossing fields in Fig. 3 for the $N=1$, 2, and 3 resonances are in moderate agreement with the oversimplified model expressed by Eq. (1) and plotted in Fig. 3 as dashed lines, which only considers the linear shift of the Stark-ladder levels relative to the last well so that the energy crossings appear equally spaced in $\mathcal{E}^{-1}$. A more realistic picture should include two additional effects: the coupling among the superlattice states ($N=1,2,3,\ldots$) and the Stark shift of the quantum levels.[10] The former is especially important for states corresponding to the high-energy edge of the miniband. This explains that the largest discrepancy between the experimental resonant fields and those predicted by Eq. (1) occurs for $N=1$, the highest-energy superlattice state. The Stark shift is proportional, to a first approximation,[11] to $m\mathcal{E}^2L^4$ (L and m are the well width and the carrier effective mass, respectively), and therefore it affects mostly the states of the last well.

To account qualitatively for the splittings and the fields at which they occur, we have modeled the heterostructure in the framework of the envelope-function approximation,[4] and solved numerically Schrödinger's equation, which automatically includes the above effects. The electron-hole interaction was ignored, except by the inclusion of a single, field-independent exciton energy of 4.5 meV, corresponding to bulk GaAs. Although, in principle, a "superlattice" consisting of only three wells would suffice to produce the observed number of resonances, such a reduced set leads to unrealistic edge effects, mainly for the $N=3$ resonance. Our calculations show that these are negligible once the number of wells is increased to five. The problem of calculating bound states in the presence of an electric field was avoided by artificially introducing infinite barriers on both sides of the structure, at a certain distance from the wells.

The calculated transition energies are represented in Fig. 3 by solid lines. The fits to both the heavy-hole and light-hole sets of transitions were optimized simultaneously by the values 1.514 eV, 1.39 V, and 3.25×10^4 cm^{-1} for

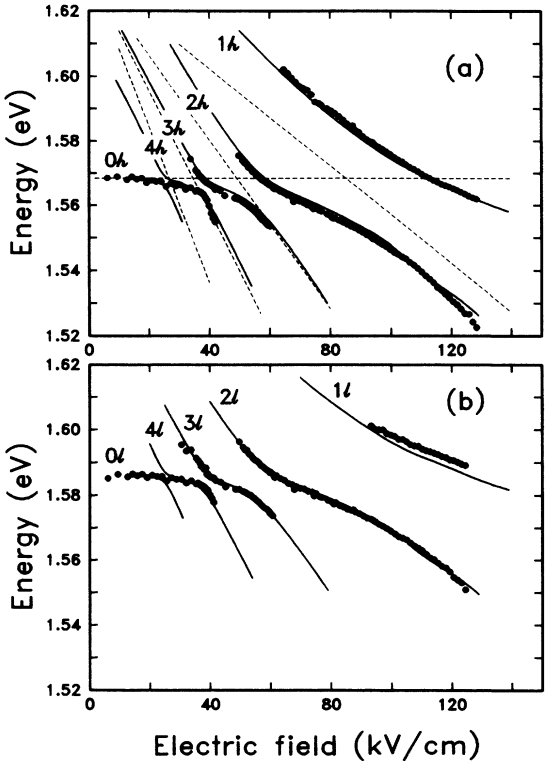

FIG. 3. Transition energies, obtained from photocurrent spectra, as a function of electric field (solid circles). Dashed lines represent energies calculated ignoring both the coupling of the superlattice states and their interaction with the localized state. Solid lines are for transition energies calculated by solving numerically Schrödinger's equation for the last well coupled to a reduced superlattice (five periods).

the excitonic band gap of GaAs, the built-in voltage, and the proportionality constant between the electric field and the external voltage, respectively. The small differences with their nominal values of 1.515 eV, 1.60 V, and 3.41×10^4 cm^{-1} probably reflect indirectly the absence in our calculation of detailed excitonic effects as well as slight departures from the intended layer thicknesses.

The excellent agreement between calculated and experimental energies in a broad range of electric fields confirms the validity of our model. Although simple, since it replaces the superlattice by a reduced number of wells (five in this case) and uses the envelope-function approximation for very narrow barriers, the model includes the most important element: the interaction of the localized state in the last well with the extended states in the superlattice, whose most direct manifestation are the large anticrossings in the energy spectrum. In principle, similar interactions would exist between the $N=0$ well and the wells in the superlattice even if these would be uncoupled among themselves. However, except for the nearest neighbor, $N=1$, the interaction would be negligibly small. For instance, the 11.9-meV gap at 48.8 kV/cm, corresponding to the $N=2$ resonance, would practically vanish in the absence of superlattice effects. The experimental observation of the $N=2$ and $N=3$ transitions provides

unambiguous evidence of the extension of the superlattice wave functions beyond the periodic region. The tunability offered by an electric field leads under resonant conditions to an enhancement of their leakage into the last well and to a mixing with its otherwise localized state.

This work has been sponsored in part by the U.S. Army Research Office (Triangle Research Park, NC). We thank L. F. Alexander for sample preparation, and J. W. Little and R. P. Leavitt for making available to us their results before publication.

---

*Present and permanent address: Instituto de Ciencia de Materiales de Madrid (CSIC), Departemento de Física Aplicada (C-IV), Universidad Autónoma de Madrid, Ciudad Universitaria de Cantoblanco, E-28049 Madrid, Spain.

†Present and permanent address: Department of Electrical Engineering, Hokkaido University, Sapporo 060, Hokkaido, Japan.

[1]I. Tamm, Phys. Z. Sowjetunion **1**, 733 (1932).

[2]H. Ohno, E. E. Mendez, J. A. Brum, J. M. Hong, F. Agulló-Rueda, L. L. Chang, and L. Esaki, Phys. Rev. Lett. **64**, 2555 (1990).

[3]E. E. Mendez, F. Agulló-Rueda, and J. M. Hong, Phys. Rev. Lett. **60**, 2426 (1988).

[4]The material parameters used in the calculations throughout this paper are the following: electron effective mass, $m_e^*/m_0 = 0.067 + 0.083x$; heavy-hole effective mass, $m_{hh}^*/m_0 = 0.340 + 0.069x$; light-hole effective mass, $m_{lh}/m_0 = 0.094 + 0.056x$; conduction-band discontinuity, $\Delta E_c = 944x$ meV; valence-band discontinuity, $\Delta E_v = 550x$ meV, where m_0 is the free-electron mass and x the AlAs mole fraction in $Ga_{1-x}Al_xAs$.

[5]H. Q. Le, J. J. Zayhowski, and W. D. Goodhue, Appl. Phys. Lett. **50**, 1518 (1987).

[6]P.-F. Yuh and K. L. Wang, Phys. Rev. B **38**, 8377 (1988).

[7]J. E. Golub, P. F. Liao, D. J. Eilenberger, J. P. Harbison, L. T. Florez, and Y. Prior, Appl. Phys. Lett. **53**, 2584 (1988).

[8]J. W. Little and R. P. Leavitt, Phys. Rev. B **39**, 1365 (1989).

[9]J. W. Little and R. P. Leavitt, Phys. Rev. B **41**, 5174 (1990).

[10]E. E. Mendez, G. Bastard, L. L. Chang, L. Esaki, H. Morkoç, and R. Fischer, Phys. Rev. B **26**, 7101 (1982).

[11]G. Bastard, E. E. Mendez, L. L. Chang, and L. Esaki, Phys. Rev. B **28**, 3241 (1983).